HOKKAIDO UNIVERSITY

Title	Enhancing biocement performance via brushite-to-hydroxyapatite transformation from waste bones
Author(s)	Yan, Zhen; Avramenko, Maksym; Nakashima, Kazunori et al.
Citation	Acta Geotechnica, 20(6), 2721-2732 https://doi.org/10.1007/s11440-025-02589-9
Issue Date	2025-06
Doc URL	https://hdl.handle.net/2115/97530
Rights	This version of the article has been accepted for publication, after peer review (when applicable) and is subject to Springer Nature’ s AM terms of use, but is not the Version of Record and does not reflect post-acceptance improvements, or any corrections. The Version of Record is available online at: http://dx.doi.org/10.1007/s11440-025-02589-9
Type	journal article
File Information	Clean-Revised Manuscript.pdf

Hokkaido University Collection of Scholarly and Academic Papers : HUSCAP

Enhancing Biocement Performance via Brushite-to-Hydroxyapatite Transformation from Waste Bones

Zhen Yan[1,*], Maksym Avramenko[1], Kazunori Nakashima[2], Chikara Takano[2], Satoru Kawasaki[2]

[1] Division of Sustainable Resources Engineering, Graduate School of Engineering, Hokkaido University, Kita 13, Nishi 8, Kita-Ku, Sapporo 060-8628, Japan

[2] Division of Sustainable Resources Engineering, Faculty of Engineering, Hokkaido University, Kita 13, Nishi 8, Kita-Ku, Sapporo 060-8628, Japan

Abstract

The use of biocement represents a sustainable and innovative approach in geotechnical engineering. However, achieving optimal results often necessitates additional treatment cycles according to the current strength models based on sediment content. This study investigates the utilization of kitchen waste bones as a sustainable source of calcium and phosphorus to enhance biocement strength through controlled phase transformations. The objective is to induce the phase transformation of sediment from brushite to hydroxyapatite by increasing temperature and pH. This transformation was verified through X-ray diffraction (XRD) and energy-dispersive spectroscopy (EDS) analyses, confirming the successful conversion of calcium phosphate phases. Compared to samples with similar sediment content, the unconfined compressive strength (UCS) of the samples subjected to phase transformation increased by more than fivefold, indicating a substantial improvement in strength within the same treatment cycles. Overall, these findings emphasize the potential of kitchen waste bones in advancing sustainable biocement practices, providing a crystal transformation solution that significantly enhances the performance of biocement.

Keywords: Biocement; Calcium phosphate; Brushite; Hydroxyapatite; Sediment content; Phase transition; Waste recycling.

1. Introduction

On a global scale, sustainable construction engineering practices are increasingly recognized as vital for combating climate change and achieving environmental objectives. The construction industry is a major contributor to global energy consumption and CO_2 emissions, with traditional portland cement production playing a significant role**[1–3]**. This has led to a growing impetus to seek more environmentally friendly alternative materials. In recent years, biocement has emerged as an innovative technology. Due to its independence from the high-temperature calcination process typically associated with cement production, biocement offers significant sustainability advantages**[4–6]**, making it highly applicable in various construction engineering projects**[7–9]**.

In practical engineering applications, there are usually specific requirements for treatment strength. In current sediment-based biocement research, the factors influencing strength improvement often focus on the amount of sediment[10–14], which typically necessitates an extended treatment cycle. However, as the number of treatments increases, the soil's permeability decreases, hindering the penetration of the treatment solution into the soil, leading to a decline in treatment effectiveness over time, thus failing to meet expected outcomes. The inefficient use of solidification solution in the later stages of treatment may result in raw material waste. Additionally, prolonged treatment cycles extend construction time and overall costs. One method to achieve better treatment outcomes without blindly increasing the number of treatments is through fiber blending**[15–17]**. It is important to note that pre-mixing fibers into the soil may cause disturbances to in-situ soils, increase construction steps, and raise costs. Moreover, the combination of biopolymers with biocement offers a new perspective**[18–20]**. However, as organic compounds, biopolymers may be degraded by indigenous bacteria in actual engineering applications, and their long-term treatment effects require further investigation.

Against this backdrop, this study proposes a method to enhance the strength of calcium phosphate biocement, not through additional treatment cycles, but by regulating temperature and pH to control the crystal structure of the sediment. Given the distinct mechanical properties of various calcium phosphate precipitates, adjustments in temperature and pH were used to induce the formation of hydroxyapatite from brushite phases within the biocement matrix. This targeted modulation of the crystal structure resulted in a more than fivefold increase in compressive strength under comparable sediment content conditions. Following the procedure illustrated in **Figure 1**, various ratios of sustainable source solidification solutions were applied at different temperatures, and the reactions were monitored during the solidification tests. After completing the solidification tests, the samples were evaluated for strength and settlement, followed by Scanning electron microscopy (SEM) analysis to examine the microstructure, and XRD and EDS analyses to identify phase composition and elemental distribution. This research not only proposes a novel approach to enhancing the strength of biotreated samples but also offers more effective and sustainable solutions for future practical applications. These findings have the potential to advance the application of biocement in construction engineering and promote the development of sustainable building materials.

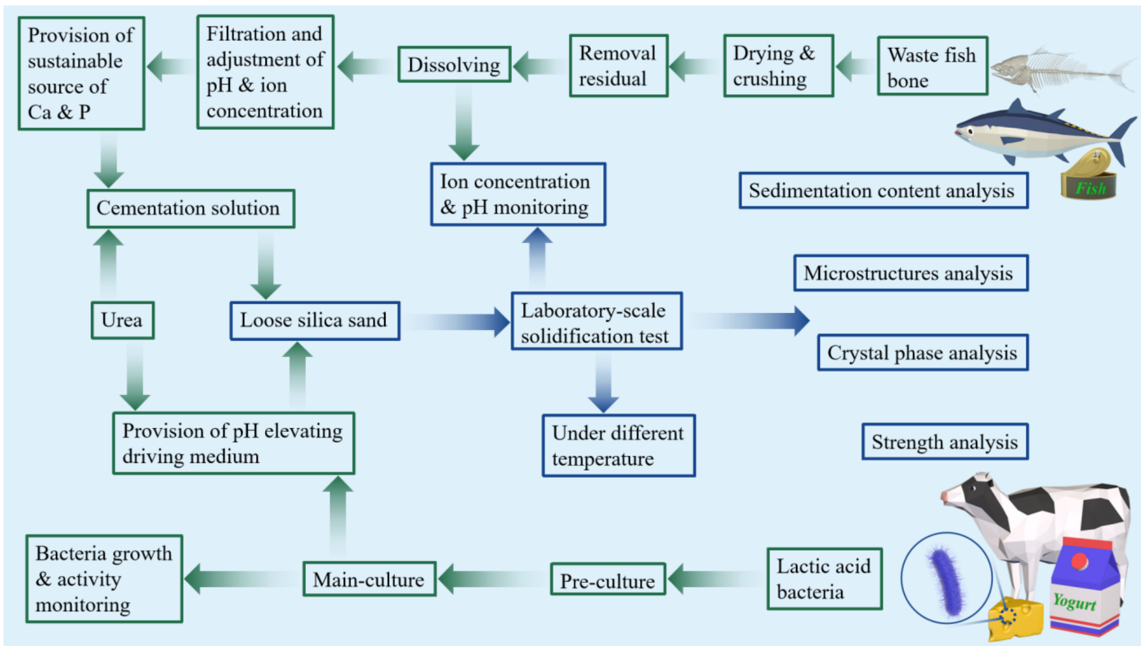

Figure1. *The main process of the experiment.*

2. Materials and methods

2.1 Bacterial cultivation and monitoring

Calcium phosphate biocement can only dissolve sufficient ions in acidic environments, thereby enabling in-situ injection. Bacteria with urease activity under acidic conditions hydrolyze urea upon injection, which raises the pH and induces the in-situ precipitation of calcium phosphate from the pre-injected acidic solution. In this study, the Gram-positive bacterium shown in Figure 2a, which exhibits urease activity under acidic conditions, was provided by the Biological Resource Center at the National Institute of Technology and Evaluation in Tokyo, Japan. The strain, NBRC 14511, belongs to the Limosilactobacillus species and is classified as Biosafety Level 1, making it a low-risk bacterium suitable for practical applications. After rehydration, the bacteria were pre-cultured and then cultured at 35 °C in Man-Rogosa-Sharpe medium, a standard nutrient medium widely used for cultivating lactic acid bacteria[21–25]. Daily measurements were taken during the main cultivation process to monitor bacterial growth and urease activity.The 1000x magnification of bacteria photographed using a Keyence VHX-500 digital microscope is shown in **Figure 2d**. Bacterial growth was measured at an optical density of 600 nm using a Jasco V-730 UV-Vis spectrophotometer. Urease activity was assessed using an AS ONE Thermal Robo TR-1α water bath, maintaining a temperature of 35°C. The activity was evaluated by measuring the amount of ammonia/ammonium produced from the hydrolysis of urea by the bacterial solution, as described in **Equations (2)** and **(3)**, over a specified reaction period. Ammonia/ammonium generated from the hydrolysis of urea reacts with hypochlorite to form chloramine. Chloramine then reacts with phenol under alkaline conditions to produce indole blue dye[26–30]. The intensity of the indole blue dye was measured at 630 nm. A calibration curve was established using ammonium chloride solutions of known concentrations and their corresponding absorbance values, allowing for the determination of ammonia/ammonium concentrations and the quantification of bacterial urease activity.

$$CO(NH_2)_2 + 2H_2O \xrightarrow{\text{urease}} H_2CO_3 + 2NH_3 \qquad \textbf{(2)}$$

$$NH_3 + H_2O \leftrightarrow OH^- + NH_4^+ \qquad \textbf{(3)}$$

2.2 Used sand and preparation of solidification solution

The initial characteristics of the soil to be treated, such as grain size and pore size distribution, relative density, and particle surface properties, determine permeability and fluid flow patterns. These characteristics can affect the distribution of bacteria and solidification solutions during the biocementation process, thereby potentially influencing treatment effectiveness. For this study, Toyoura sand, as shown in **Figure 2c**, was selected due to its physical uniformity, which minimizes the potential complex effects on the biocementation process. Toyoura sand has a soil particle density of 2.64 g/cm³, a maximum void ratio of 0.973, and a minimum void ratio of 0.609. The uniformity coefficient is 1.30, and the curvature coefficient is 0.96. The sieve analysis depicted in **Figure 2b** confirms that this sand is poorly graded, with fairly uniform particle sizes and low fine content. The SEM image in **Figure 2f** reveals that the particle shapes range from angular to sub-angular, and the XRD analysis in **Figure 2h** indicates that its crystalline phase is primarily quartz.

In this study, kitchen waste fish bones obtained from the local market were used as a green source of calcium and phosphorus for the solidification solution. As shown in **Figure 2e**, their main component is hydroxyapatite. The preparation process is illustrated in the flowchart in **Figure 1**. Specifically, the bones were first dried at room temperature and then crushed into fragments smaller than 1 cm for the subsequent experiments. The fragments were then boiled in a 2% NaOH solution for 30 minutes to thoroughly remove attached organic matter such as grease. After filtering, the clean fish bones were dissolved in a 1% HCl solution as **Equation (1)**, stirred at 1000 rpm to extract calcium and phosphorus ions from the bones, as shown in **Figure 2g**. The solution was then filtered, and its pH and calcium ion concentration were adjusted to approximately pH 3.0 (±0.1) and 10,000 (±100) ppm, respectively. Finally, urea was added to the solidification solution according to the different groups listed in **Table 1**.

$$Ca_5(PO_4)_3OH + 4HCl \rightarrow 5Ca^{2+} + 3HPO_4^{2-} + 4Cl^- + H_2O \quad \textbf{(1)}$$

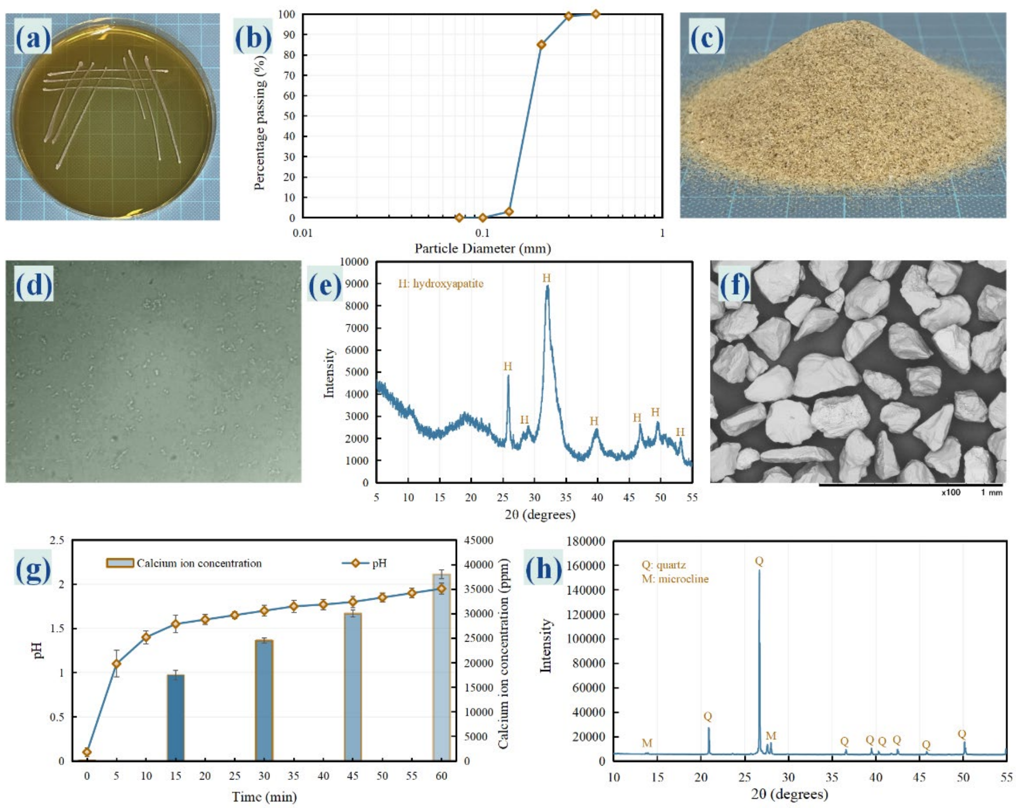

***Figure 2**: (a) shows the appearance of the cultured bacteria used, (b) displays the particle size distribution of the sand used, (c) illustrates the appearance of the sand used, (d) provides a microscopic magnification of the bacteria used, (e) presents the XRD analysis of the bones used, (f) depicts the SEM image of the sand used, (g) details the pH and calcium ion monitoring during the preparation of the solidification solution, (h) exhibits the XRD image of the sand used.*

2.3 Laboratory-scale sand solidification tests

Laboratory-scale solidification studies utilized syringes as simplified molds. Pre-washed and oven-dried sand was loaded into the molds and compacted. Filter paper was placed at the bottom of the sand to prevent loss of sand during the experiments. The experimental procedure based on initial trials is shown in Table 1, with each of the three replicates conducted for 14 days. Each day, 10 mL of solidification solution, mixed with varying amounts of urea according to the experimental design, was injected in a single dose. Bacterial solution of 10 mL was introduced on Day 1 and Day 8, two hours prior to the injection of the solidification solution. After injecting the solidification or bacterial solution from the top of the mold, gravity and capillary action alone were relied upon to infiltrate the sand. The bottom clamps were fully opened to allow the solidification solution to flow out, thereby simulating the unsaturated conditions that may occur in actual treatment processes. Samples were collected every 24 hours to monitor the pH value using a Horiba LAQUA F-71 benchtop pH meter and the calcium ion concentration using a Horiba LAQUAtwin Ca-11 compact calcium ion meter in the effluent. By comparing the initial calcium ion concentration of the solidification solution with the effluent measurements, the calcium ion consumption rate was determined. At the end of the solidification experiment, 100 mL of distilled water was added to each sample to wash out any unreacted chemicals. The samples were then dried in an oven at 60 °C for 48 hours to ensure complete dryness. After drying, the molds were carefully cut open, and subsequent tests were conducted on the samples.

***Table 1**: Formulations of the samples in the solidification tests.*

Case name	Incubation temperature (°C)	Treatment duration (day)	Urea/ Ca^{2+} ratio	Concentration of urea (mol/L)	Concentration of Ca^{2+} (mol/L)	Amount of bacteria solution (mL)	Amount of cementation solution (mL)
1A	25	14	0	0	0.25	10*2	10*14
1B			0.5	0.125	0.25	10*2	10*14
1C			1	0.25	0.25	10*2	10*14
1D			2	0.5	0.25	10*2	10*14
2A	30	14	0	0	0.25	10*2	10*14
2B			0.5	0.125	0.25	10*2	10*14
2C			1	0.25	0.25	10*2	10*14
2D			2	0.5	0.25	10*2	10*14
3A	35	14	0	0	0.25	10*2	10*14
3B			0.5	0.125	0.25	10*2	10*14
3C			1	0.25	0.25	10*2	10*14
3D			2	0.5	0.25	10*2	10*14

2.4 Characterization

The strength of samples treated with biological cement is a critical parameter for evaluating the efficacy of the solidification process. Due to the irregular shape of the samples, the top and bottom sections were trimmed, and any loose parts caused by the demolding process were removed to ensure uniform dimensions of approximately 4 cm and consistent positioning for all test specimens. This was accomplished using a penetration test with the SH-70 permeameter a widely employed instrument for evaluating the strength of soft rocks and stabilized soils in both field and laboratory settings. In three repeated tests, each sample was tested at five different locations, and the average UCS value was recorded.

The sediment content was quantified using an acid digestion method. Specifically, a sufficient amount of 1 % hydrochloric acid was mixed with a known quantity of the sample to dissolve the sediment. After 24 hours, the sample was rinsed with distilled water and dried in an oven at 60 °C. The sediment amount was calculated based on the mass difference of the sample before and after the acid treatment.

The microstructural features of the samples were examined through SEM using Hitachi TM3000 microscope. To further elucidate the crystalline structure of the solidified samples, phase analysis was performed with a MultiFlex X-ray Diffractometer utilizing a Cu K-alpha source and a scanning rate of 6.5 °/min. Additionally, EDS was conducted with a JEOL JSM-IT200 to provide detailed elemental distribution.

3. Results and discussion

3.1. Monitoring of bacterial activity and solidification process

Figure 3a illustrates the monitoring results of urease activity in the cultured bacteria. The results indicate that the urease activity reached its peak platform from about the 7th day. Consequently, this cultivation period was selected for subsequent solidification tests to achieve optimal efficiency.

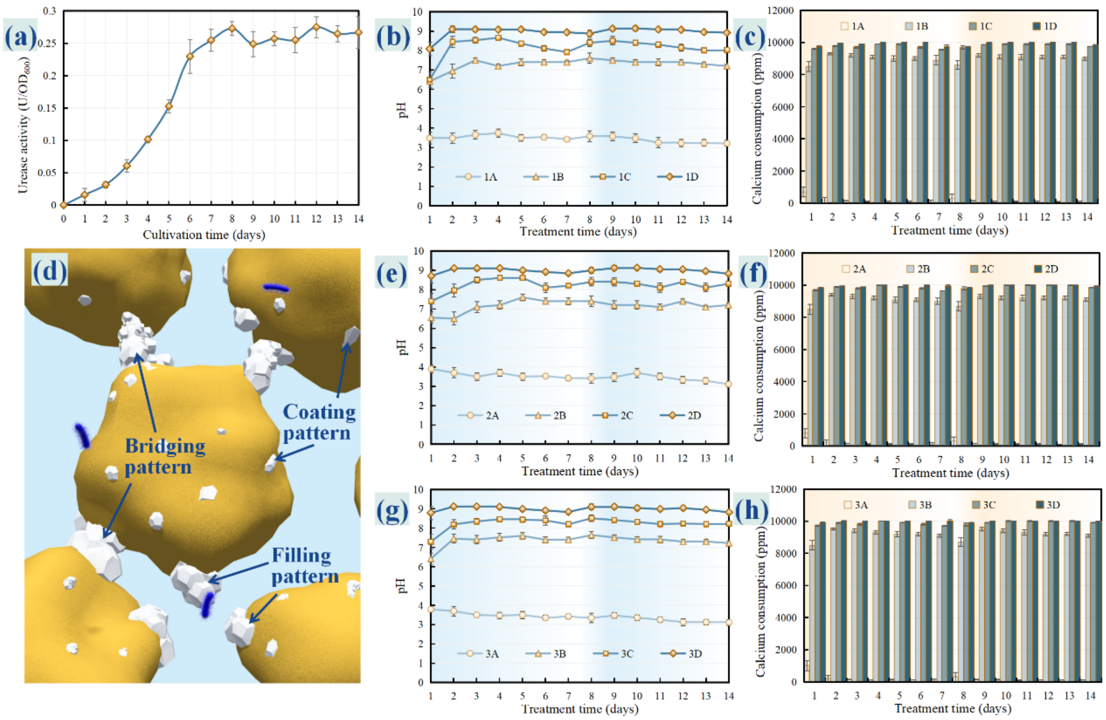

***Figure 3**: (a) shows the activity monitoring of the bacteria during cultivation, (b), (e), and (g) present the pH monitoring during the solidification tests, (c), (f), and (h) illustrate the calcium ion consumption during the solidification tests, and (d) depicts a schematic diagram of the solidification mechanism.*

Figure 3b, **e**, **g** depict the pH monitoring during the solidification tests. The initial pH of the solidification solution was 3.0, and the rise in the pH of the effluent is attributed to bacterial urea hydrolysis, as outlined in **Equation (2)** and **(3)**. The magnitude of this increase is related to the amount of urea added. At a ratio of 2.0, the pH reached its maximum; as the ratio decreased, so did the pH. Notably, there were slight fluctuations in pH at the beginning and on the 8th day, likely due to the introduction of new bacteria. Moreover, the pH did not significantly vary across different temperatures during the solidification tests.

Figures 3c, **f**, and **h** show the variation in Ca^{2+} consumption over time during the solidification process. Following urea hydrolysis, the pH of the solidification solution increases, reducing the solubility of calcium phosphate and leading to precipitation[31–35], as described by the mechanism in **Equation (4)**. Therefore, the consumption of calcium ions is also related to the urea/Ca^{2+} ratio. At a ratio of 2.0 and 1.0, calcium ions are almost entirely consumed; at ratios of 0.5, the consumption is slightly lower. As illustrated in the mechanism diagram in **Figure 3d**, the consumed calcium ions form sediment that bind the sand particles, thus achieving solidification.

$$Ca^{2+} + HPO_4^{2-} + 2H_2O \rightarrow CaHPO_4 \cdot 2H_2O \qquad \textbf{(4)}$$

3.2.Evaluation of solidification effects

Figures 4a, **d**, and **g** provide a visual representation of the appearance of the specimens after solidification. **Figures 4b** illustrates the results of the sediment content in the samples. At the same temperature, the sediment content trends showing an increasing trend with varying urea concentrations. The control group, which did not contain urea, showed no notable increase in sediment content, whereas the Groups 0.5, 1, and 2 had substantial amounts of sediment that were comparable. At different temperatures, the trend of sediment content variation is consistent with the previous trend of calcium ion consumption, showing no significant differences. Notably, sample 1D achieved the highest sediment content of 6.85% at 25 ℃, while sample 3D was slightly lower at 6.34% at 35 ℃, which may be attributed to the influence of lower temperatures potentially contributing to higher sediment content[36].

Figures 4e also presents the UCS results of the samples. The strength of the Groups 0.5, 1 and 2 reached above 1 MPa. Remarkably, at 35 ℃, the strength of Group 2 was significantly higher than that of the other specimens with similar amounts of sediment, reaching up to 12.95 MPa. Previous studies have indicated that, with the same aggregate particle size, the primary factor influencing the UCS of biocemented specimens is the amount of sediment. This suggests that other factors affecting UCS strength may be present, which will be analyzed in the subsequent section.

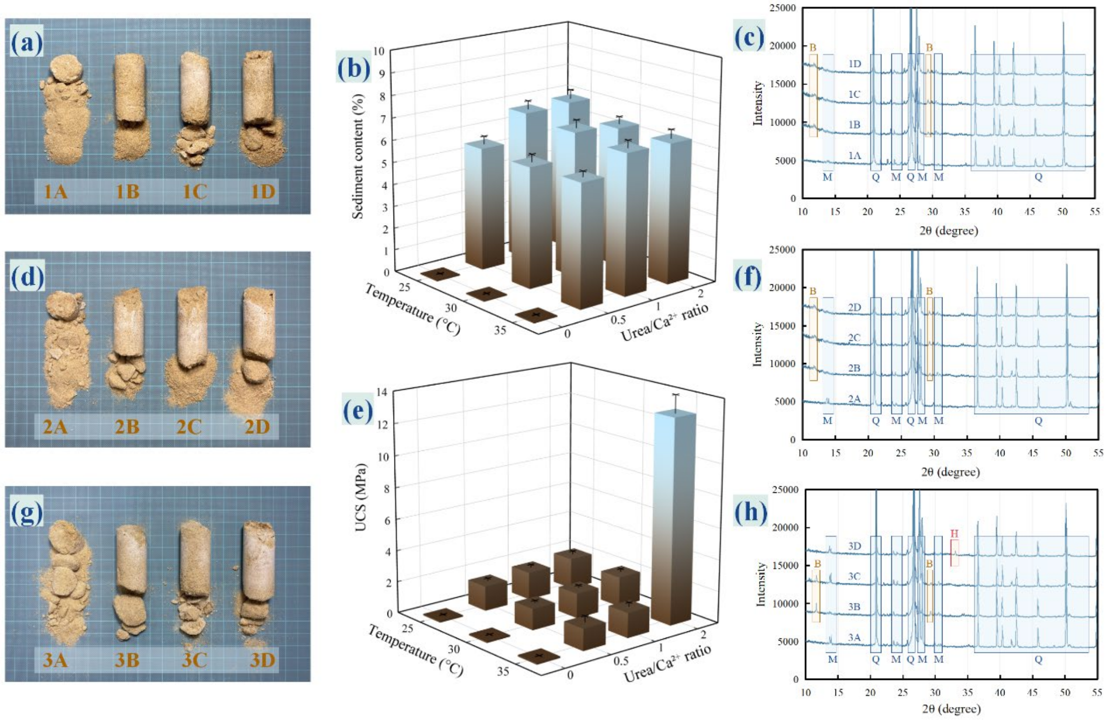

***Figure 4**: (a), (d), and (g) show the appearance of the samples after solidification tests, (b) and (e) display the distribution of Sediment content and UCS, and (c), (f), and (h) present the XRD analysis of the samples after solidification tests.*

3.3. Microstructural and crystal phase inspection

Changes in the microstructure of specimens often influence macroscopic properties, including strength. **Figure 5** displays SEM images of all specimens to assess microstructural features and sediment morphology. The sediment patterns in biocement typically affect its strength[37–41], with bridging patterns contributing significantly to strength enhancement, and coating patterns also providing some improvement[42, 43]. It can be observed that, except for the control group, the remaining specimens exhibit both the bridging patterns between soil particles, as indicated by the circles, and the coating patterns on the particle surfaces, as indicated by the rectangles. Therefore, sediment morphology does not appear to be the primary reason for the high strength observed in specimen 3D.

$$5\ CaHPO_4 \cdot 2\ H_2O + 4\ OH^- \rightarrow Ca_5(PO_4)_3OH + 2\ HPO_4^{2-} + 13\ H_2O \qquad \textbf{(5)}$$

Studies have shown that brushite can act as a precursor and transform into the more stable hydroxyapatite[44–46], as illustrated in **Equation (5)**. Combining the XRD results presented in Figures 4c, f, and h, where Q stands for quartz, M stands for microcline, B stands for brushite, and H stands for hydroxyapatite, it is apparent that the calcium phosphate sediments shown in the other samples are brushite, whereas those depicted in sample 3D are hydroxyapatite. The formation of calcium phosphate sediment in the samples is often influenced by temperature and pH adjustments[47–51], leading to the transformation of metastable brushite into the more stable hydroxyapatite over time. Hydroxyapatite possesses a hexagonal crystal structure, whereas brushite exhibits a monoclinic crystal structure. This structural difference may explain why hydroxyapatite exhibits superior mechanical strength compared to brushite[52], which may account for the higher strength observed in specimen 3D, despite it containing the similar amount of sediment as the other specimens. Similarly, current studies using tests such as nanoindentation have found that in calcium carbonate-based biocements, the cementing properties and micro-mechanical performance of $CaCO_3$ precipitates are related to their crystal composition[53]. A higher content of calcite improves the adhesion of calcium carbonate precipitates. Calcite exhibits better mechanical properties, including elastic modulus, hardness, and ductility, compared to aragonite. Therefore, it is also necessary to conduct further experiments in the future to deepen the understanding of the characteristics and mechanical performance of brushite and hydroxyapatite.

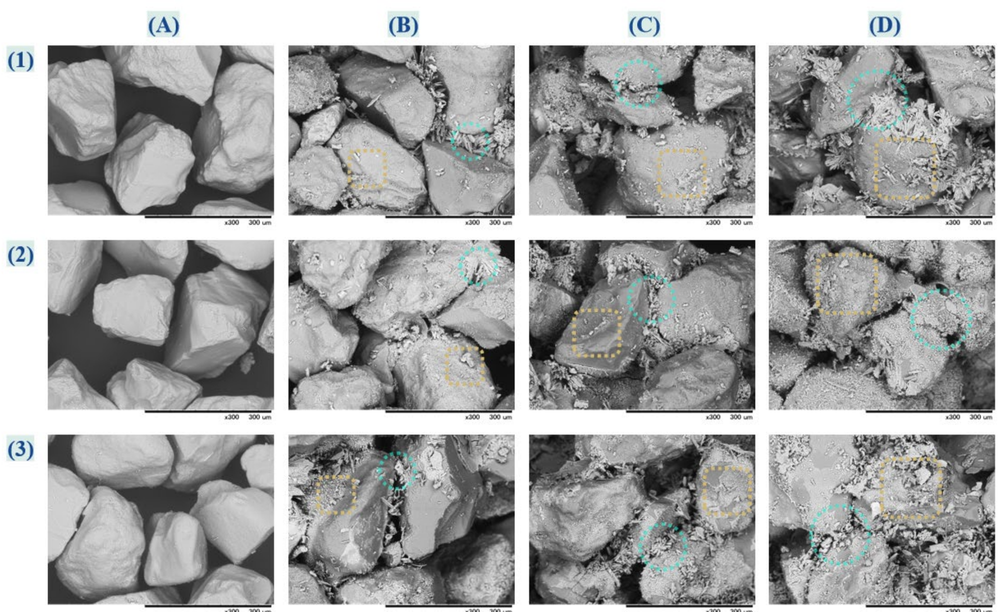

***Figure 5**: Displays the SEM analysis of the samples after the solidification tests. The numbers on the left and letters at the top correspond to the sample identifiers.*

Figure 6 shows the elemental distribution of phosphorus, calcium, and silicon as analyzed by EDS, the labels Si, Ca, and P at the top indicate the distribution of the corresponding elements. During the analysis, Si was used to differentiate sand grains, while Ca and P represent the distribution of biocement components. **Figure 6a** shows the untreated quartz sand, which only shows intensity for Si with no detectable Ca or P. In **Figure 6b** and **c**, the distribution areas for Ca and P are comparably bright, while in **Figure 6d**, the brightness of the P region is significantly lower than that of the Ca region. This suggests that the abundance of phosphorus in the sediment in **Figure 6d** is lower compared to other figures, the chemical composition of the sediment in **Figure 6d** may differ from those in **Figure 6b** and **c**. Given that the ideal P/Ca ratio for hydroxyapatite is 0.6, which is lower than the ideal P/Ca ratio of 1 for brushite, this further confirms the presence of hydroxyapatite in sample 3D.

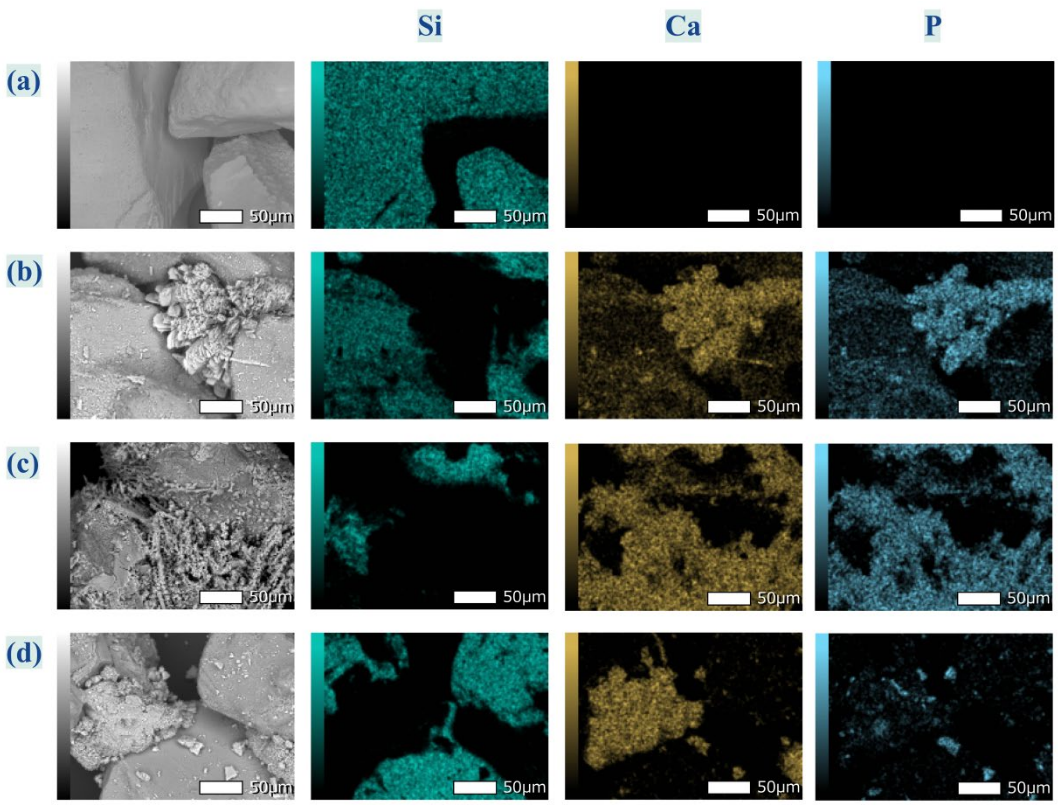

Figure 6*: (a) shows the EDS analysis of the sand used. (b), (c), and (d) display the EDS analysis of the 1D, 2D, and 3D samples after solidification tests, respectively.*

3.4. Environmental impact and future application analysis

When scaling up the application on site as shown in **Figure 7**, it is essential to consider their environmental friendliness and sustainability. The sustainable calcium sources for biocement, including construction waste, eggshells, and shellfish waste[54–58], have been investigated and applied. In this study, biocement based on calcium phosphate utilizes both calcium and phosphorus sources derived from fish bones from kitchen waste. With societal development and the expansion of the food industry, a significant quantity of bones has become an important waste in the food sector[59–63]. Therefore, this study represents a novel approach to the sustainable utilization of bone waste. Utilizing waste bones not only addresses the waste problem generated by the food industry but also provides a cost-effective raw material for biocement production. This option reduces waste management costs, reflects the principles of a circular economy, helps lower costs, and promotes the large-scale application of biocement.

Moreover, despite the induced crystal phase change achieving a strength in 3D samples that was more than five times higher than that of other samples with similar sediment content, further research is needed to quantitatively evaluate crystal configuration factors and develop appropriate fitting functions. The relatively high temperatures required for the crystal transformation in this study may be geographically limited for large-scale applications, and the preparation, storage and injection of the acidic solidification solution are also challenging. Therefore, this method may not always be suitable for field applications. Future research should explore additional methods for altering crystal phases, such as adjusting the calcium/phosphorus ratio in the solidification solution, to improve the practicality and efficiency of this method under varying environmental conditions.

Furthermore, animal urine produced in livestock farming can serve as a sustainable source of urea for biocement production[64–68]. Utilizing animal urine effectively mitigates the environmental impact of animal manure, and avoids the energy-intensive and environmentally harmful issues associated with synthetic urea production[69–73]. This practice contributes to resource recycling and reduces the environmental burden of the production process. Future research should focus on comprehensive lifecycle assessments and sustainability studies to systematically evaluate the economic costs, carbon footprint, and environmental impacts of this approach[74–78], providing a scientific basis for the promotion of biocement in various application scenarios.

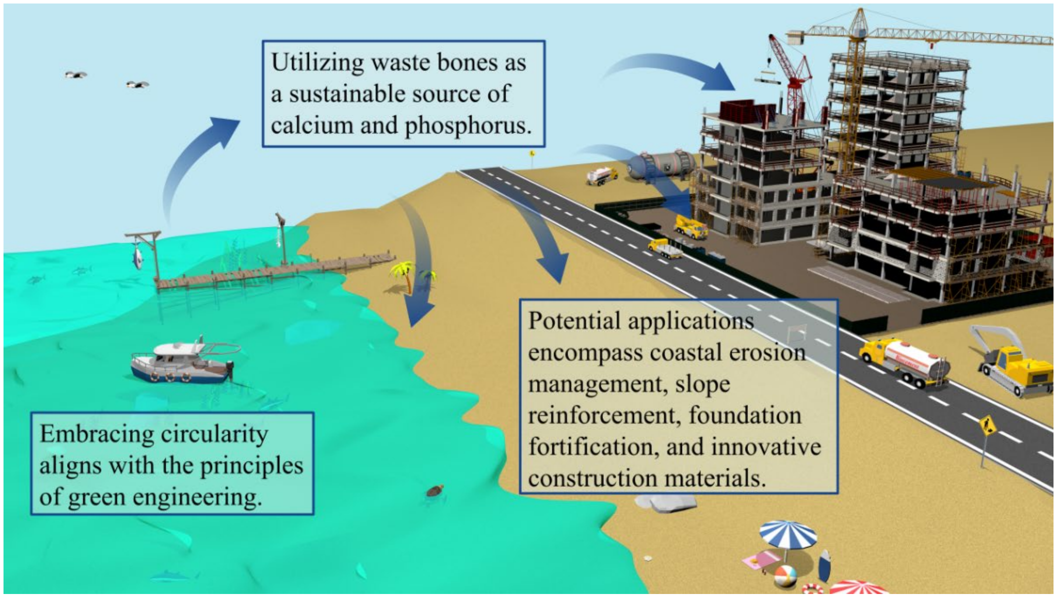

***Figure** 7: Illustrates potential future applications.*

4. Conclusion

This study aimed to enhance the strength of biocement derived from kitchen waste bones by inducing crystallographic changes through temperature variation. The key findings are as follows:

1. The use of food waste bones as a sustainable source for biocement has been validated, which helps in reducing both the costs of food waste disposal and the costs of biocement production.

2. Evidence provided by XRD and EDS has demonstrated crystallographic changes from brushite to hydroxyapatite, resulting in more than a fivefold increase in strength at the similar sediment levels.

3. Future research should continue to explore this study to gain a deeper understanding. This includes investigating and quantitatively considering the contribution of crystal structure factors to strength, establishing corresponding fitting functions, and exploring other methods for altering the crystalline phase, such as adjusting the calcium-to-phosphorus ratio in the solidification

solution to enhance the practicality and efficiency of this method under different environmental conditions.

5. References:

1. Ige OE, Von Kallon DV, Desai D (2024) Carbon emissions mitigation methods for cement industry using a systems dynamics model. Clean Technol Environ Policy 26:579–597. https://doi.org/10.1007/s10098-023-02683-0
2. Benhelal E, Shamsaei E, Rashid MI (2021) Challenges against CO2 abatement strategies in cement industry: A review. J Environ Sci 104:84–101. https://doi.org/10.1016/j.jes.2020.11.020
3. Ali MB, Saidur R, Hossain MS (2011) A review on emission analysis in cement industries. Renew Sustain Energy Rev 15:2252–2261. https://doi.org/10.1016/j.rser.2011.02.014
4. Nur MMA, Dewi RN (2024) Opportunities and challenges of microalgae in biocement production and self-repair mechanisms. Biocatal Agric Biotechnol 56:103048. https://doi.org/10.1016/j.bcab.2024.103048
5. Alemu D, Demiss W, Korsa G (2022) Bacterial Performance in Crack Healing and its Role in Creating Sustainable Construction. Int J Microbiol 2022:6907314. https://doi.org/10.1155/2022/6907314
6. Achal V, Mukherjee A, Kumari D, Zhang Q (2015) Biomineralization for sustainable construction – A review of processes and applications. Earth-Sci Rev 148:1–17. https://doi.org/10.1016/j.earscirev.2015.05.008
7. He J, Liu Y, Liu L, et al (2023) Recent development on optimization of bio-cementation for soil stabilization and wind erosion control. Biogeotechnics 1:100022. https://doi.org/10.1016/j.bgtech.2023.100022
8. Dubey AA, Dhami NK, Ravi K, Mukherjee A (2023) Erosion mitigation with biocementation: a review on applications, challenges, & future perspectives. Rev Environ Sci Biotechnol 22:1059–1091. https://doi.org/10.1007/s11157-023-09674-z
9. Seifan M, Samani AK, Berenjian A (2016) Bioconcrete: next generation of self-healing concrete. Appl Microbiol Biotechnol 100:2591–2602. https://doi.org/10.1007/s00253-016-7316-z
10. Khoshdel Sangdeh M, Salimi M, Hakimi Khansar H, et al (2024) Predicting the precipitated calcium carbonate and unconfined compressive strength of bio-mediated sands through robust hybrid optimization algorithms. Transp Geotech 46:101235. https://doi.org/10.1016/j.trgeo.2024.101235
11. Wang H, Sun X, Miao L, et al (2023) Garlic extract addition for soil improvement at various temperatures using enzyme-induced carbonate precipitation (EICP) method. J Rock Mech Geotech Eng 15:3230–3243. https://doi.org/10.1016/j.jrmge.2023.03.018
12. Liu J, Li X, Liu X, et al (2023) Mechanical Properties of Eolian Sand Solidified by Microbially Induced Calcium Carbonate Precipitation (MICP). Geomicrobiol J 40:688–698. https://doi.org/10.1080/01490451.2023.2235345
13. Ahenkorah I, Rahman MM, Karim MR, Beecham S (2021) Enzyme induced calcium carbonate precipitation and its engineering application: A systematic review and meta-analysis. Constr Build Mater 308:125000. https://doi.org/10.1016/j.conbuildmat.2021.125000
14. Choi S-G, Chang I, Lee M, et al (2020) Review on geotechnical engineering properties of sands treated by microbially induced calcium carbonate precipitation (MICP) and biopolymers. Constr Build Mater 246:118415. https://doi.org/10.1016/j.conbuildmat.2020.118415
15. Tang C-S, Li H, Pan X-H, et al (2022) Coupling effect of biocementation-fiber reinforcement on mechanical behavior of calcareous sand for ocean engineering. Bull Eng Geol Environ 81:163. https://doi.org/10.1007/s10064-022-02662-7

16. Kou H-L, Liu J-H, Zhang P, et al (2022) Ecofriendly improvement of coastal calcareous sandy slope using recycled shredded coconut coir (RSC) and bio-cement. Acta Geotech 17:5375–5389. https://doi.org/10.1007/s11440-022-01560-2

17. Yao D, Wu J, Wang G, et al (2021) Effect of wool fiber addition on the reinforcement of loose sands by microbially induced carbonate precipitation (MICP): mechanical property and underlying mechanism. Acta Geotech 16:1401–1416. https://doi.org/10.1007/s11440-020-01112-6

18. Hang L, Van Paassen LA, Ehsasi F, et al (2024) An Experimental Investigation on Use of Xanthan Gum Biopolymer as Additive for Improving the Reinforcement Effect of Biocementation on Sandy Soils. Geomicrobiol J 41:627–635. https://doi.org/10.1080/01490451.2024.2360476

19. Miyake M, Kim D, Hata T (2022) Casein-assisted enhancement of the compressive strength of biocemented sand. Sci Rep 12:12754. https://doi.org/10.1038/s41598-022-16879-9

20. Dubey AA, Hooper-Lewis J, Ravi K, et al (2022) Biopolymer-biocement composite treatment for stabilisation of soil against both current and wave erosion. Acta Geotech 17:5391–5410. https://doi.org/10.1007/s11440-022-01536-2

21. Meruvu H, Harsa ST (2023) Lactic acid bacteria: isolation–characterization approaches and industrial applications. Crit Rev Food Sci Nutr 63:8337–8356. https://doi.org/10.1080/10408398.2022.2054936

22. Renschler MA, Wyatt A, Anene N, et al (2020) Using nitrous acid-modified de Man, Rogosa, and Sharpe medium to selectively isolate and culture lactic acid bacteria from dairy foods. J Dairy Sci 103:1215–1222. https://doi.org/10.3168/jds.2019-17041

23. Colombo M, Castilho NPA, Todorov SD, Nero LA (2018) Beneficial properties of lactic acid bacteria naturally present in dairy production. BMC Microbiol 18:219. https://doi.org/10.1186/s12866-018-1356-8

24. Özcelik S, Kuley E, Özogul F (2016) Formation of lactic, acetic, succinic, propionic, formic and butyric acid by lactic acid bacteria. LWT 73:536–542. https://doi.org/10.1016/j.lwt.2016.06.066

25. Sathe SJ, Nawani NN, Dhakephalkar PK, Kapadnis BP (2007) Antifungal lactic acid bacteria with potential to prolong shelf-life of fresh vegetables. J Appl Microbiol 103:2622–2628. https://doi.org/10.1111/j.1365-2672.2007.03525.x

26. Li D, Xu X, Li Z, et al (2020) Detection methods of ammonia nitrogen in water: A review. TrAC Trends Anal Chem 127:115890. https://doi.org/10.1016/j.trac.2020.115890

27. Zhu Y, Chen J, Yuan D, et al (2019) Development of analytical methods for ammonium determination in seawater over the last two decades. TrAC Trends Anal Chem 119:115627. https://doi.org/10.1016/j.trac.2019.115627

28. Ma J, Li P, Lin K, et al (2018) Optimization of a salinity-interference-free indophenol method for the determination of ammonium in natural waters using *o*-phenylphenol. Talanta 179:608–614. https://doi.org/10.1016/j.talanta.2017.11.069

29. Lin K, Li P, Wu Q, et al (2018) Automated determination of ammonium in natural waters with reverse flow injection analysis based on the indophenol blue method with *o*-phenylphenol. Microchem J 138:519–525. https://doi.org/10.1016/j.microc.2018.02.004

30. Tzollas NM, Zachariadis GA, Anthemidis AN, Stratis JA (2010) A new approach to indophenol blue method for determination of ammonium in geothermal waters with high mineral content. Int J Environ Anal Chem 90:115–126. https://doi.org/10.1080/03067310902962528

31. Avramenko M, Nakashima K, Takano C, Kawasaki S (2024) Ecofriendly solidification of sand using microbially induced calcium phosphate precipitation. Sci Rep 14:12412. https://doi.org/10.1038/s41598-024-63016-9

32. Avramenko M, Nakashima K, Takano C, Kawasaki S (2023) Eco-friendly soil stabilization method using fish bone as cement material. Sci Total Environ 900:165823. https://doi.org/10.1016/j.scitotenv.2023.165823

33. Avramenko M, Nakashima K, Kawasaki S (2022) State-of-the-Art Review on Engineering Uses of Calcium Phosphate Compounds: An Eco-Friendly Approach for Soil Improvement. Materials 15:6878. https://doi.org/10.3390/ma15196878
34. Gowthaman S, Yamamoto M, Nakashima K, et al (2021) Calcium phosphate biocement using bone meal and acid urease: An eco-friendly approach for soil improvement. J Clean Prod 319:128782. https://doi.org/10.1016/j.jclepro.2021.128782
35. Ivanov V, Stabnikov V, Kawasaki S (2019) Ecofriendly calcium phosphate and calcium bicarbonate biogrouts. J Clean Prod 218:328–334. https://doi.org/10.1016/j.jclepro.2019.01.315
36. Xiao Y, Wang Y, Wang S, et al (2021) Homogeneity and mechanical behaviors of sands improved by a temperature-controlled one-phase MICP method. Acta Geotech 16:1417–1427. https://doi.org/10.1007/s11440-020-01122-4
37. Yan Z, Nakashima K, Takano C, Kawasaki S (2024) Feasibility study of enhancing enzyme-induced carbonate precipitation with eggshell waste for sand solidification. Biogeotechnics 2:100108. https://doi.org/10.1016/j.bgtech.2024.100108
38. Zhang Q, Ye W, Liu Z, et al (2023) Influence of injection methods on calcareous sand cementation by EICP technique. Constr Build Mater 363:129724. https://doi.org/10.1016/j.conbuildmat.2022.129724
39. Almajed A, Abbas H, Arab M, et al (2020) Enzyme-Induced Carbonate Precipitation (EICP)-Based methods for ecofriendly stabilization of different types of natural sands. J Clean Prod 274:122627. https://doi.org/10.1016/j.jclepro.2020.122627
40. Xiao Y, Stuedlein AW, Ran J, et al (2019) Effect of Particle Shape on Strength and Stiffness of Biocemented Glass Beads. J Geotech Geoenvironmental Eng 145:06019016. https://doi.org/10.1061/(ASCE)GT.1943-5606.0002165
41. Terzis D, Laloui L (2018) 3-D micro-architecture and mechanical response of soil cemented via microbial-induced calcite precipitation. Sci Rep 8:1416. https://doi.org/10.1038/s41598-018-19895-w
42. Wu H, Wu W, Liang W, et al (2023) 3D DEM modeling of biocemented sand with fines as cementing agents. Int J Numer Anal Methods Geomech 47:212–240. https://doi.org/10.1002/nag.3466
43. DeJong JT, Mortensen BM, Martinez BC, Nelson DC (2010) Bio-mediated soil improvement. Ecol Eng 36:197–210. https://doi.org/10.1016/j.ecoleng.2008.12.029
44. Ucar S, Bjørnøy SH, Bassett DC, et al (2017) Transformation of brushite to hydroxyapatite and effects of alginate additives. J Cryst Growth 468:774–780. https://doi.org/10.1016/j.jcrysgro.2016.11.019
45. Dorozhkin SV, Epple M (2002) Biological and Medical Significance of Calcium Phosphates. Angew Chem Int Ed 41:3130–3146. https://doi.org/10.1002/1521-3773(20020902)41:17<3130::AID-ANIE3130>3.0.CO;2-1
46. Kumar M, Dasarathy H, Riley C (1999) Electrodeposition of brushite coatings and their transformation to hydroxyapatite in aqueous solutions. J Biomed Mater Res 45:302–310. https://doi.org/10.1002/(SICI)1097-4636(19990615)45:4<302::AID-JBM4>3.0.CO;2-A
47. Zhang J, Wang L, Putnis CV (2019) Underlying Role of Brushite in Pathological Mineralization of Hydroxyapatite. J Phys Chem B 123:2874–2881. https://doi.org/10.1021/acs.jpcb.9b00728
48. Rocha DN da, Silva MHP da, Campos JB de, et al (2018) Kinetics of conversion of brushite coatings to hydroxyapatite in alkaline solution. J Mater Res Technol 7:479–486. https://doi.org/10.1016/j.jmrt.2018.02.002
49. Engstrand J, Persson C, Engqvist H (2014) The effect of composition on mechanical properties of brushite cements. J Mech Behav Biomed Mater 29:81–90. https://doi.org/10.1016/j.jmbbm.2013.08.024

50. Štulajterová R, Medvecký Ľ (2008) Effect of calcium ions on transformation brushite to hydroxyapatite in aqueous solutions. Colloids Surf Physicochem Eng Asp 316:104–109. https://doi.org/10.1016/j.colsurfa.2007.08.036
51. Furutaka K, Monma H, Okura T, Takahashi S (2006) Characteristic reaction processes in the system brushite–NaOH solution. J Eur Ceram Soc 26:543–547. https://doi.org/10.1016/j.jeurceramsoc.2005.07.016
52. Charrière E, Terrazzoni S, Pittet C, et al (2001) Mechanical characterization of brushite and hydroxyapatite cements. Biomaterials 22:2937–2945. https://doi.org/10.1016/S0142-9612(01)00041-2
53. Xu K, Huang M, Cui M, Li S (2024) Effect of crystal morphology on cementability and micromechanical properties of calcium carbonate precipitate induced by crude soybean enzyme. J Rock Mech Geotech Eng 16:5095–5108. https://doi.org/10.1016/j.jrmge.2023.08.024
54. Yu X, Chu J, Wu S, Wang K (2023) Production of biocement using steel slag. Constr Build Mater 383:131365. https://doi.org/10.1016/j.conbuildmat.2023.131365
55. Sujiritha PB, Vikash VL, Antony GS, et al (2022) Valorization of tannery solid wastes for sustainable enzyme induced carbonate precipitation process. Chemosphere 308:136533. https://doi.org/10.1016/j.chemosphere.2022.136533
56. Kulanthaivel P, Soundara B, Selvakumar S, Das A (2022) Application of waste eggshell as a source of calcium in bacterial bio-cementation to enhance the engineering characteristics of sand. Environ Sci Pollut Res 29:66450–66461. https://doi.org/10.1007/s11356-022-20484-8
57. Liang S, Chen J, Niu J, et al (2020) Using recycled calcium sources to solidify sandy soil through microbial induced carbonate precipitation. Mar Georesources Geotechnol 38:393–399. https://doi.org/10.1080/1064119X.2019.1575939
58. Choi SG, Chu J, Brown RC, et al (2017) Sustainable Biocement Production via Microbially Induced Calcium Carbonate Precipitation: Use of Limestone and Acetic Acid Derived from Pyrolysis of Lignocellulosic Biomass. ACS Sustain Chem Eng 5:5183–5190. https://doi.org/10.1021/acssuschemeng.7b00521
59. Huyen DT, Phat LN, Long DH, et al (2024) Investigation of characteristics and application of food waste-derived bone char on plant growth. J Environ Chem Eng 12:113446. https://doi.org/10.1016/j.jece.2024.113446
60. Hart A, Ebiundu K, Peretomode E, et al (2022) Value-added materials recovered from waste bone biomass: technologies and applications. RSC Adv 12:22302–22330. https://doi.org/10.1039/D2RA03557J
61. Kowalski Z, Kulczycka J, Makara A, Harazin P (2021) Quantification of material recovery from meat waste incineration – An approach to an updated food waste hierarchy. J Hazard Mater 416:126021. https://doi.org/10.1016/j.jhazmat.2021.126021
62. Toldrá F, Mora L, Reig M (2016) New insights into meat by-product utilization. Meat Sci 120:54–59. https://doi.org/10.1016/j.meatsci.2016.04.021
63. Arvanitoyannis IS, Ladas D (2008) Meat waste treatment methods and potential uses. Int J Food Sci Technol 43:543–559. https://doi.org/10.1111/j.1365-2621.2006.01492.x
64. Yang Y, Chu J, Cheng L, Liu H (2022) Utilization of carbide sludge and urine for sustainable biocement production. J Environ Chem Eng 10:107443. https://doi.org/10.1016/j.jece.2022.107443
65. Crane L, Ray H, Hamdan N, Boyer TH (2022) Enzyme-induced carbonate precipitation utilizing fresh urine and calcium-rich zeolites. J Environ Chem Eng 10:107238. https://doi.org/10.1016/j.jece.2022.107238
66. Comadran-Casas C, Schaschke CJ, Akunna JC, Jorat ME (2022) Cow urine as a source of nutrients for Microbial-Induced Calcite Precipitation in sandy soil. J Environ Manage 304:114307. https://doi.org/10.1016/j.jenvman.2021.114307

67. Lambert SE, Randall DG (2019) Manufacturing bio-bricks using microbial induced calcium carbonate precipitation and human urine. Water Res 160:158–166. https://doi.org/10.1016/j.watres.2019.05.069

68. Chen H-J, Huang Y-H, Chen C-C, et al (2019) Microbial Induced Calcium Carbonate Precipitation (MICP) Using Pig Urine as an Alternative to Industrial Urea. Waste Biomass Valorization 10:2887–2895. https://doi.org/10.1007/s12649-018-0324-8

69. Masjedi SK, Kazemi A, Moeinnadini M, et al (2024) Urea production: An absolute environmental sustainability assessment. Sci Total Environ 908:168225. https://doi.org/10.1016/j.scitotenv.2023.168225

70. Galusnyak SC, Petrescu L, Sandu V-C, Cormos C-C (2023) Environmental impact assessment of green ammonia coupled with urea and ammonium nitrate production. J Environ Manage 343:118215. https://doi.org/10.1016/j.jenvman.2023.118215

71. Mei Z, Zhou Y, Lv W, et al (2022) Recent Progress in Electrocatalytic Urea Synthesis under Ambient Conditions. ACS Sustain Chem Eng 10:12477–12496. https://doi.org/10.1021/acssuschemeng.2c03681

72. Zhang H, Wang L, Van herle J, et al (2021) Techno-economic comparison of 100% renewable urea production processes. Appl Energy 284:116401. https://doi.org/10.1016/j.apenergy.2020.116401

73. Chen C, Zhu X, Wen X, et al (2020) Coupling N2 and CO2 in H2O to synthesize urea under ambient conditions. Nat Chem 12:717–724. https://doi.org/10.1038/s41557-020-0481-9

74. Alotaibi E, Arab MG, Abdallah M, et al (2022) Life cycle assessment of biocemented sands using enzyme induced carbonate precipitation (EICP) for soil stabilization applications. Sci Rep 12:6032. https://doi.org/10.1038/s41598-022-09723-7

75. Al-Gheethi AA, Memon ZA, Balasbaneh AT, et al (2022) Critical Analysis for Life Cycle Assessment of Bio-Cementitious Materials Production and Sustainable Solutions. Sustainability 14:1920. https://doi.org/10.3390/su14031920

76. Raymond AJ, Kendall A, DeJong JT, et al (2021) Life Cycle Sustainability Assessment of Fugitive Dust Control Methods. J Constr Eng Manag 147:04020181. https://doi.org/10.1061/(ASCE)CO.1943-7862.0001993

77. Porter H, Mukherjee A, Tuladhar R, Dhami NK (2021) Life Cycle Assessment of Biocement: An Emerging Sustainable Solution? Sustainability 13:13878. https://doi.org/10.3390/su132413878

78. Deng X, Li Y, Liu H, et al (2021) Examining Energy Consumption and Carbon Emissions of Microbial Induced Carbonate Precipitation Using the Life Cycle Assessment Method. Sustainability 13:4856. https://doi.org/10.3390/su13094856

Acknowledgements

This work was supported by JSPS KAKENHI Grant Number JP22H01581, and was partly supported by JST SPRING, Grant Number JPMJSP2119.

Declaration of competing interest

The authors declare that they have no known competing financial interests or personal relationships that could have appeared to influence the work reported in this paper.

Data statement

All the experimental data that support the findings of this study are available from the corresponding author upon reasonable request through email.